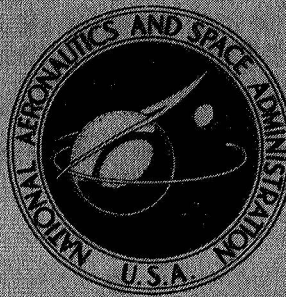


**NASA TECHNICAL
MEMORANDUM**



NASA TM X-2673

NASA TM X-2673

**CASE FILE
COPY**

**THERMAL CORRECTION OF
DEFORMATIONS IN A TELESCOPE MIRROR**

by Marvin D. Rhodes

*Langley Research Center
Hampton, Va. 23365*

NATIONAL AERONAUTICS AND SPACE ADMINISTRATION • WASHINGTON, D. C. • JANUARY 1973

1. Report No. NASA TM X-2673	2. Government Accession No.	3. Recipient's Catalog No.	
4. Title and Subtitle THERMAL CORRECTION OF DEFORMATIONS IN A TELESCOPE MIRROR		5. Report Date December 1972	
		6. Performing Organization Code	
7. Author(s) Marvin D. Rhodes		8. Performing Organization Report No. L-8360	
		10. Work Unit No. 502-32-02-04	
9. Performing Organization Name and Address NASA Langley Research Center Hampton, Va. 23365		11. Contract or Grant No.	
		13. Type of Report and Period Covered Technical Memorandum	
12. Sponsoring Agency Name and Address National Aeronautics and Space Administration Washington, D.C. 20546		14. Sponsoring Agency Code	
15. Supplementary Notes The information presented herein was included in a thesis entitled "Thermal Active Optics Technique for Correcting Symmetrical Distortions in Space Telescope Mirrors" submitted in partial fulfillment of the requirements for the degree of Master of Science in Mechanical Engineering, University of Virginia, Charlottesville, Virginia, September 1970.			
16. Abstract <p>Orbiting astronomical observatories have the potential for making observations far superior to those from earth-based mirrors. In order for this performance to be realized, the contour of the primary mirror must be very accurately controlled. A preliminary investigation of the use of thermally induced elastic strains for correcting axisymmetric deformations in space telescope mirrors has been presented. The relation between axial deformation and thermal inputs was determined by a finite-difference solution of the equations for thin elastic shells.</p> <p>The use of this technique was demonstrated analytically on a beryllium paraboloid. This mirror had 10 equally spaced thermal inputs and results are presented which show the nature of the temperature distribution required to correct deformations due to an acceleration-type loading.</p>			
17. Key Words (Suggested by Author(s)) Telescopes Active controls Thermal distortions		18. Distribution Statement Unclassified - Unlimited	
19. Security Classif. (of this report) Unclassified	20. Security Classif. (of this page) Unclassified	21. No. of Pages 19	22. Price* \$3.00

THERMAL CORRECTION OF DEFORMATIONS IN A TELESCOPE MIRROR*

By Marvin D. Rhodes
Langley Research Center

SUMMARY

Orbiting astronomical observatories have the potential for making observations far superior to those from earth-based mirrors. In order for this performance to be realized, the contour of the primary mirror must be very accurately controlled. A preliminary investigation of the use of thermally induced elastic strains for correcting axisymmetric deformations in space telescope mirrors has been presented. The relation between axial deformation and thermal inputs was determined by a finite-difference solution of the equations for thin elastic shells.

The use of this technique was demonstrated analytically on a beryllium paraboloid. This mirror had 10 equally spaced thermal inputs and results are presented which show the nature of the temperature distribution required to correct deformations due to an acceleration-type loading.

INTRODUCTION

Orbiting astronomical observatories have two potential advantages over earth-based telescopes (ref. 1): first, the entire electromagnetic spectrum is available for observation of stellar sources, and second, orbiting astronomical observatories will not be affected by air turbulence which limits the resolution of earth-based telescopes. Away from this turbulence the resolution of astronomical observations will be increased by at least 1 order of magnitude, which will permit telescope operation near the diffraction limit (ref. 2).

Several studies of space telescopes have been conducted and all have recommended the use of a Cassegrainian optical system (refs. 3 and 4). These studies indicated that the primary mirror is the critical element in this system and deviations from the design shape must be controlled to extremely close tolerances. If close tolerances cannot be maintained, the resolution of space telescopes may be no better than earth-based observatories and their usefulness will be severely restricted.

*The information presented herein was included in a thesis entitled "Thermal Active Optics Technique for Correcting Symmetrical Distortions in Space Telescope Mirrors" submitted in partial fulfillment of the requirements for the degree of Master of Science in Mechanical Engineering, University of Virginia, Charlottesville, Virginia, September 1970.

Two types of primary mirrors have been proposed for use in space telescopes (ref. 5). The first type is a passive mirror which would be designed to retain the proper contour without correction for the life of the telescope. This design may not be feasible since intolerable deformations may be caused by the relaxation of residual stresses. Also, actual launch and space environmental loads on the mirror are difficult to predict. The second type of primary mirror is known as an active optics system and uses a relatively thin mirror which is permitted to deform moderately under operational loads. A figure error sensor would monitor the deformations and activate a closed-loop control system to apply corrective loads to remove the deformations.

One active optics system which uses an array of force actuators in conjunction with a closed-loop control system to provide the corrective loads has been investigated analytically. This system has been experimentally verified (ref. 6) by using a thin, deformable, spherical mirror 76.2 cm in diameter. Another type of active control system that has been considered uses elastic deformations introduced by differential heating to maintain the proper contour. A limited thermal system has been successfully used on the earth-based telescope mirror of the Observatoire de Haute Provence (ref. 7). In the present paper a computer numerical analysis for predicting axisymmetric, thermally induced, corrective deformations in a primary mirror surface is presented. This analysis makes use of stored influence coefficients of deformations due to unit thermal inputs at various locations. The influence coefficients used herein were obtained from a finite-difference, linear shell analysis. The present analysis is demonstrated on a sample mirror configuration and the merits of two patterns of thermal inputs are investigated. In addition, the temperature distribution necessary to correct deformations from a constant acceleration loading is presented.

SYMBOLS

The units used for physical quantities defined in this paper are given in the International System of Units (SI). Factors relating this system with the U.S. Customary Units are presented in reference 8.

A	amplitude of applied temperature distribution
c	coefficients of flexibility matrix
D	diameter of telescope mirror
f	focal length of paraboloidal telescope mirror

k	coefficients of stiffness matrix
R	principal radius of curvature of paraboloidal shell middle surface
r	radial coordinate
r_m	radius of telescope mirror
T	applied temperature distribution at reference surface of mirror
α	coefficient of linear thermal expansion
Δ	meridional distance, see figure 4
δ	deformation of middle surface of shell in axial direction
δ_a	allowable deformation, $0.05 \mu\text{m}$
ξ	coordinate measured along shell meridian
ω	principal curvature of middle surface of paraboloidal shell

Subscripts:

ij	deformation at point i due to a unit load at point j
n	maximum number of control points
θ	circumferential direction
ξ	meridional direction

GENERAL CHARACTERISTICS OF THERMAL ACTIVE OPTICS SYSTEMS

A sketch of a typical earth orbiting space telescope is shown in figure 1. This model is similar to the type discussed in reference 3. The basic configuration consists of two cylindrical shells which are attached to the telescope cabin. The cylindrical shells enclose the main optical elements which are the primary and secondary mirrors. Attached to the outer shell is a system of doors that prevents sunlight from falling on the

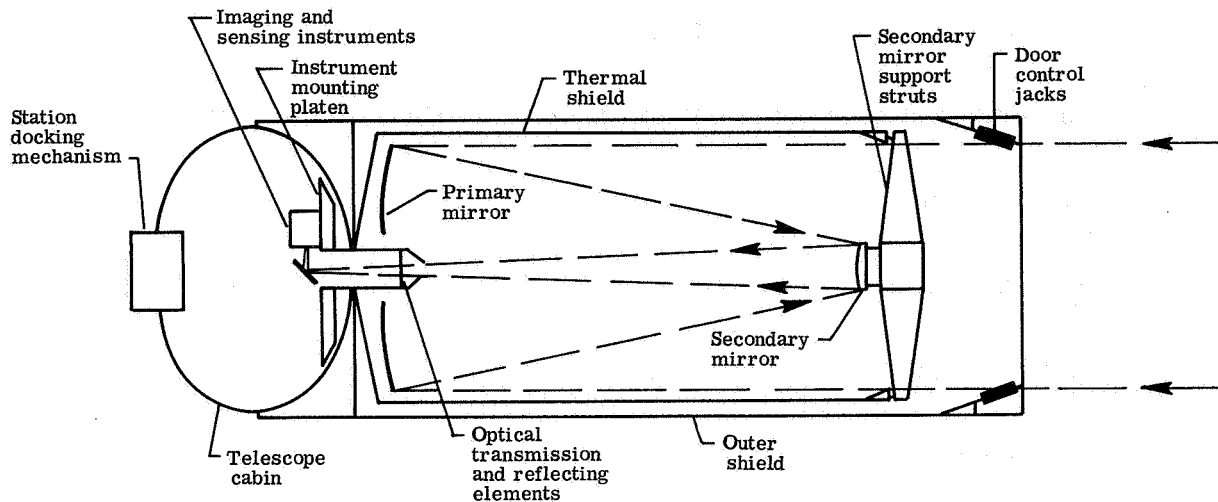


Figure 1.- Sketch of an earth orbiting space telescope.

optical system during maneuvers. The inner shell is a thermal shield to reduce solar heating loads on the primary mirror. All optical imaging devices and sensing instruments are contained in the telescope cabin. The cabin provides the necessary environment for manned support.

A schematic of a thermal active optics closed-loop control system is shown in figure 2. A complete description of a similar system utilizing force actuators can be found

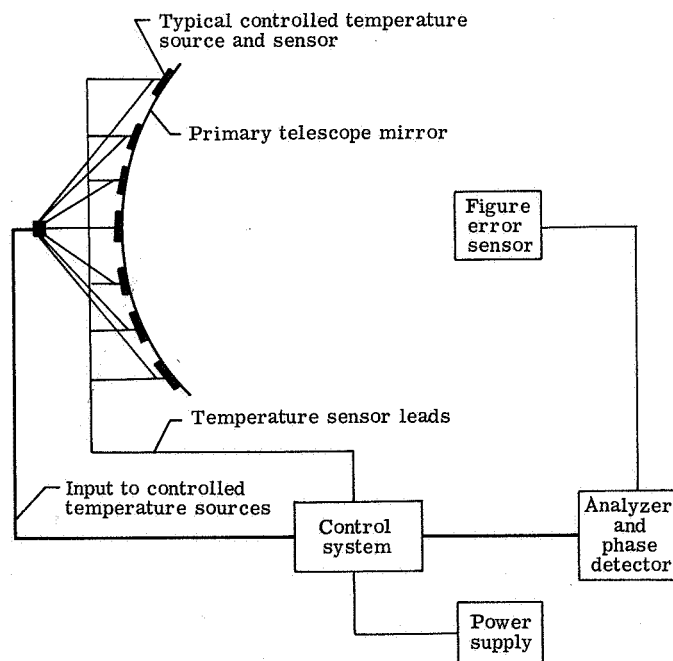


Figure 2.- Schematic of thermal active optics closed-loop control system.

in reference 6. In the present report, the primary telescope mirror is a thin parabolic shell of revolution. Deformations in this mirror are detected by a figure error sensor by using interferometric techniques. An analyzer then calculates the instantaneous amplitude of the temperature at the control stations necessary to correct the deformations. An acceptable level of distortion will depend upon the wavelength of the light being viewed and upon the desired resolution.

In general, thermal loads, that is, controlled temperature inputs, may be applied by conduction pads attached to the rear surface or by circulating fluid through channels in the interior of the mirror. For proper control and distribution, both heating and cooling loads may be necessary. Therefore, such a control system would probably be used in conjunction with a heat exchanger system. To correct asymmetric deformations the area over which the thermal load is applied will vary with the radial and circumferential location of the control station. The area and location of actuators for discrete control of linear systems has been previously investigated and is reported in reference 9. The location of error sensors has also been examined in reference 9.

SAMPLE MIRROR CONFIGURATION AND LOADING

Mirror Geometry and Properties

In order to demonstrate the use of a thermal optics control system an analytical model was established. A sketch of the mirror used in this analysis is shown in figure 3. The mirror is a thin paraboloidal shell having a focal-length—diameter ratio (f/D) of 4:1. This value is within the range of f/D currently being considered for space telescopes. Since no firm design of the telescope has been formulated, certain assumptions concerning

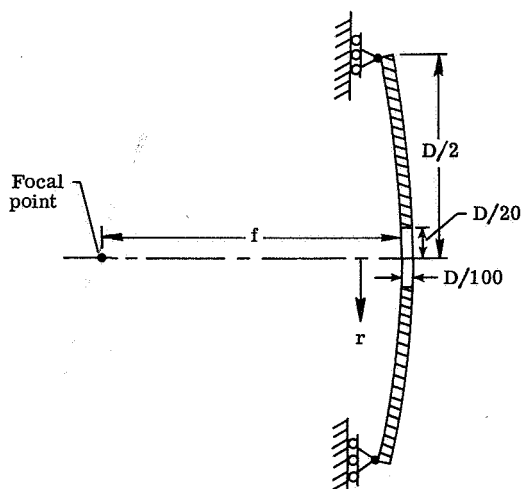


Figure 3.- Sketch of cross section of paraboloidal telescope mirror.

the mirror geometry were necessary. For example, the diameter of the central hole will depend upon the telescope optical system and manufacturing consideration. The hole was assumed to have a diameter equal to 1/10 the diameter of the mirror. In the weightless environment of space, only a very thin reflective surface would be necessary for the primary mirror. However, practical considerations of manufacture and launch will require the mirror to be sufficiently thick to withstand grinding, polishing, and handling in a gravity environment. For this investigation the thickness of the mirror was 1/100 of the diameter (ref. 5). The thickness was assumed to be constant in both circumferential and meridional directions.

Metal mirrors are ideally suited for thin one-piece construction because they have high stiffness-weight ratios. Beryllium has one of the highest stiffness-weight ratios of any structural metal and is currently being considered as a prime candidate for telescope mirror construction (ref. 10). The material properties and dimensions for this mirror are shown in table I. This material was considered to be both homogeneous and isotropic in this analysis.

TABLE I. - MATERIAL PROPERTIES AND DIMENSIONS
OF BERYLLIUM MIRROR

Property	Value
Modulus of elasticity, GN/m ²	276
Poisson's ratio	0.08
Coefficient of thermal expansion, α , K ⁻¹	1.24×10^{-5}
Diameter, D, m	3.0
Focal length, f, m	12.0
Thickness, cm	3.0

The mirror was restrained in the axial direction and unrestrained in the radial direction at the outer edge (fig. 3). This support system is similar to the three-point tangent bar mounting suspension considered in reference 3. The central cutout portion of the mirror was unrestrained.

Assumed Thermal-Active Control System

For illustrative purposes, only steady-state symmetrical deformations of the primary mirror were considered. As indicated previously, an acceptable level of deflection will depend upon the wavelength of the light source being viewed and the desired resolution. For this analysis a maximum allowable deformation of 0.1 wavelength of light was selected (ref. 3).

Ten points along the meridian of the mirror were selected as the control stations for the thermal loads. These thermal loads are rotationally symmetric about the shell axis. The use of more control stations would only have generated a larger matrix of influence coefficients and would have added little to the demonstration of the technique. For an actual control system a larger number of stations may be desirable to increase the mirror quality. Sources with a controlled temperature distribution were selected to provide the thermal inputs. The controlled sources were applied to the reference surface of the mirror. In order to simplify the problem, only steady-state deformations were examined.

Two control patterns were considered. In one pattern the control stations were equally spaced along the meridian and in the second they were located in equal annular areas.

The controlled temperature sources applied to the reference surface of the mirror were assumed to have the form

$$T_i = \begin{cases} A \left[\frac{1}{2} + \frac{1}{2} \cos \frac{\pi(\xi - \xi_i)}{\Delta/4} \right] & \left(|\xi - \xi_i| \leq \frac{\Delta}{4} \right) \\ 0 & \left(|\xi - \xi_i| > \frac{\Delta}{4} \right) \end{cases} \quad (1)$$

where $i = 1, 2, \dots, 10$. A sketch of these sources applied at a typical control station on the mirror surface is shown in figure 4. Sources of this form were chosen because they represent a compromise between a realistic thermal load and one that is simple enough to demonstrate the analytical approach. The application of this thermal input will result in two-dimensional heat flow within the mirror interior. However, a preliminary examination has indicated that the interior temperature will not be significantly different from the applied back surface distribution.

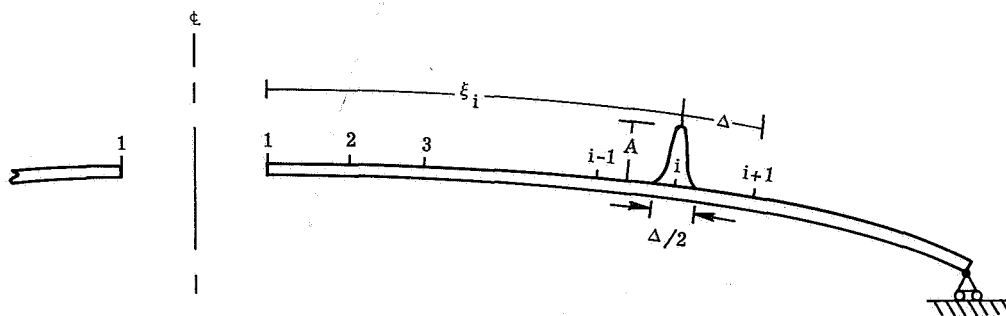


Figure 4.- Temperature distribution applied at control points along back surface of mirror for equal meridional spacing.

METHOD OF ANALYSIS

In order to determine the influence of the thermal inputs it was assumed that deformations in the primary mirror are small and that linear shell analysis is applicable. The use of linear shell theory permits the application of the principle of superposition. Consequently the deformation at the stations may be expressed as a function of the applied thermal loads by the following linear equations:

$$\left. \begin{aligned} \delta_1 &= c_{11}T_1 + c_{12}T_2 + \dots + c_{1n}T_n \\ \delta_2 &= c_{21}T_1 + c_{22}T_2 + \dots + c_{2n}T_n \\ &\vdots \\ \delta_n &= c_{n1}T_1 + c_{n2}T_2 + \dots + c_{nn}T_n \end{aligned} \right\} \quad (2)$$

The influence coefficients c_{ij} specify the contribution of each temperature distribution T_j to the deflection δ_i at the control point i . These equations may be written in the more convenient matrix notation as

$$|\delta| = [c]|T| \quad (3)$$

The square matrix $[c]$ is the flexibility matrix and the component terms are deflection influence coefficients.

The thermal loads necessary to correct mirror deflections can be expressed by inverting the flexibility matrix and multiplying by the measured deformations. Thus

$$|T| = [k]|\delta| \quad (4)$$

where

$$[k] = [c]^{-1}$$

and $[k]$ is a thermal stiffness matrix. In order for the active optics system to perform properly it is necessary to determine accurately the coefficient k_{ij} for each control point and store the coefficients in the system analyzer.

The deflection influence coefficients c_{ij} may be determined either by direct experimental tests or by analytical methods. In this investigation an analytical approach was used. The analysis is based on linear shell theory of Sanders (ref. 11). A method of

solution using finite differences is outlined in reference 12 and a computer program using this approach was coded in reference 13. This program was chosen for this analysis because it has general application and has been experimentally verified in reference 14. The program has the capability of accommodating 502 finite-difference stations along the shell meridian. Although the program is capable of including a large number of thermal control stations, only 10 stations were used, and each thermal load was permitted to span several node points in the finite-difference analysis. The midpoint of the thermal input may be selected as the control station for correction by the figure error sensor in the active control system. The temperature input necessary for the correction of any given deflection is, therefore, the amplitude of the same distribution used to determine the flexibility matrix.

Using the computer program, the deformation at station i due to the application of a unit thermal input at station j was determined. The coefficients of this equation were determined as follows. Assume that the station of interest is number 1; then assign a unit amplitude (A in eqs. (1)) to T_1 and zero to T_2, T_3, \dots, T_{10} so that equation (2) reduces to

$$\left. \begin{array}{l} \delta_1 = c_{11} \\ \delta_2 = c_{21} \\ \delta_3 = c_{31} \\ \vdots \\ \delta_{10} = c_{101} \end{array} \right\} \quad (5)$$

By applying a unit amplitude at each station separately and by calculating the resulting deflections with the computer program, each column of coefficients was determined.

In order to adapt the computer program for use in this analysis, it was necessary to write subroutines describing the shell geometry and the thermal loading. The parameters necessary to describe the shell geometry are r , $\frac{1}{r} \frac{dr}{d\xi}$, ω_θ , ω_ξ , and $\frac{d\omega_\xi}{d\xi}$. Equations describing these parameters were formulated as follows:

$$\xi = \frac{r}{2} \sqrt{\frac{r^2}{4f^2} + 1} + f \ln \left(\frac{r}{2f} + \sqrt{\frac{r^2}{4f^2} + 1} \right) \quad (6)$$

$$\omega_\theta = \frac{1}{R_\theta} = \frac{1}{\sqrt{4f^2 + r^2}} \quad (7)$$

$$\omega_{\xi} = \frac{1}{R_{\xi}} = \frac{4f^2}{(4f^2 + r^2)^{3/2}} \quad (8)$$

$$\frac{d\omega_{\xi}}{d\xi} = - \frac{24rf^3}{(4f^2 + r^2)^3} \quad (9)$$

$$\frac{1}{r} \frac{dr}{d\xi} = \frac{2f}{r\sqrt{r^2 + 4f^2}} \quad (10)$$

The program requires that the shell middle surface be defined by $r = r(\xi)$. An explicit relation for r indicated in equation (10) cannot readily be written. Therefore, it was necessary to program $r(\xi)$ by using a fourth-order Runge-Kutta approximation. The subroutine INPUT defining $r(\xi)$ and the other shell parameters is given in appendix A.

During the present investigation it was noted that some errors had been made in programing the thermal load terms presented in reference 13. These terms were in the subroutine FORCE. These terms were reprogramed and are included in the revised subroutine FORCE given in appendix B.

RESULTS AND DISCUSSION

Deformation Sensitivity to Temperature Distribution

Two patterns of control stations for the controlled temperature sources were investigated. These patterns were for an equal meridional spacing and for an equal annular area spacing. The axial deflection at each of the 10 control stations for equal meridional spacing is shown in figure 5. These curves illustrate the deflection due to the application of a thermal input of unit amplitude at each station in turn as indicated in the figure. The deformations are a maximum at the inner unrestrained boundary (except for control station 7) and decrease uniformly to zero at the axially restrained outer boundary. It was noted previously that the tolerance criterion selected for this analysis was 0.1 wavelength. At a wavelength of $0.5 \mu\text{m}$, this mirror would have an allowable deformation δ_a of $0.05 \mu\text{m}$. The deformation created by a unit thermal input at station 10 is the largest and is nearly 600 times the allowable level. The axial deformation at each of the control stations for equal area spacing is shown in figure 6. These curves are similar to those shown for equal meridional spacing. With this spacing configuration, the maximum deformation created by a unit thermal input is larger than for meridional spacing and is over 700 times the allowable level.

The deflection influence coefficients were determined for both spacing configurations from the analytical data used to plot the curves shown in figures 5 and 6. These

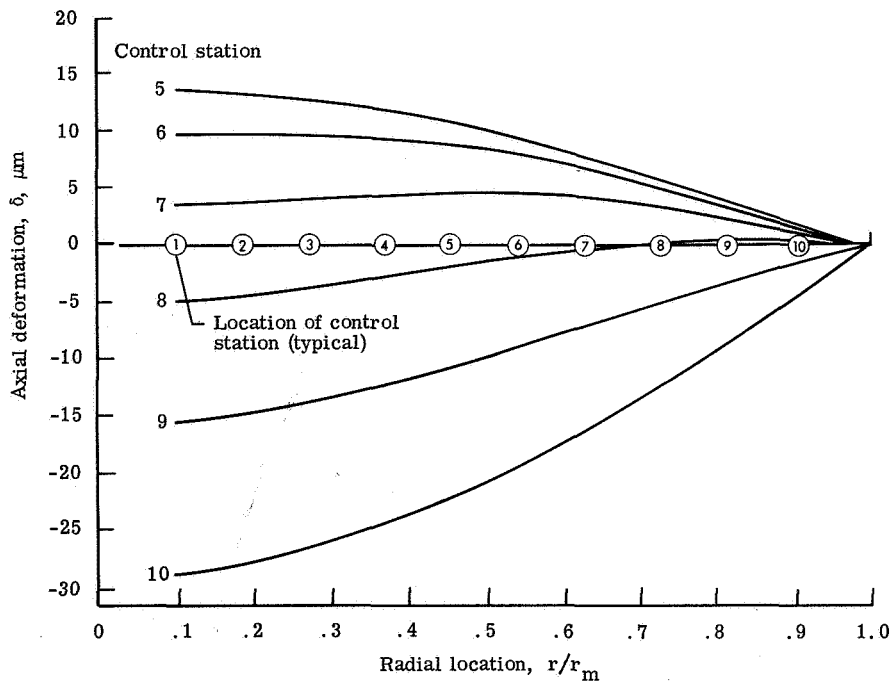
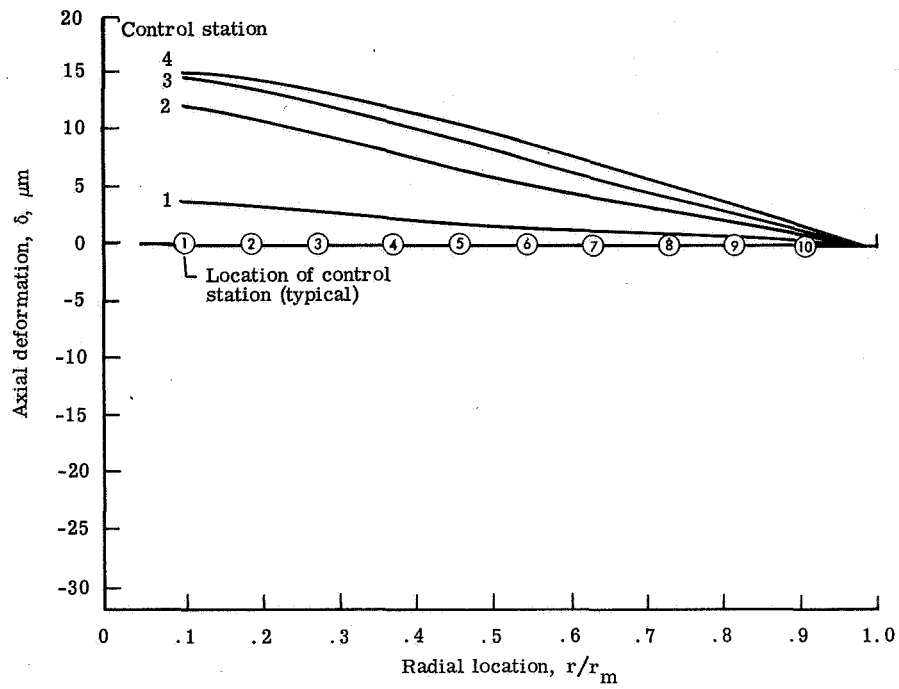


Figure 5.- Axial deformation due to unit amplitude thermal input applied individually at equal meridional spacing.

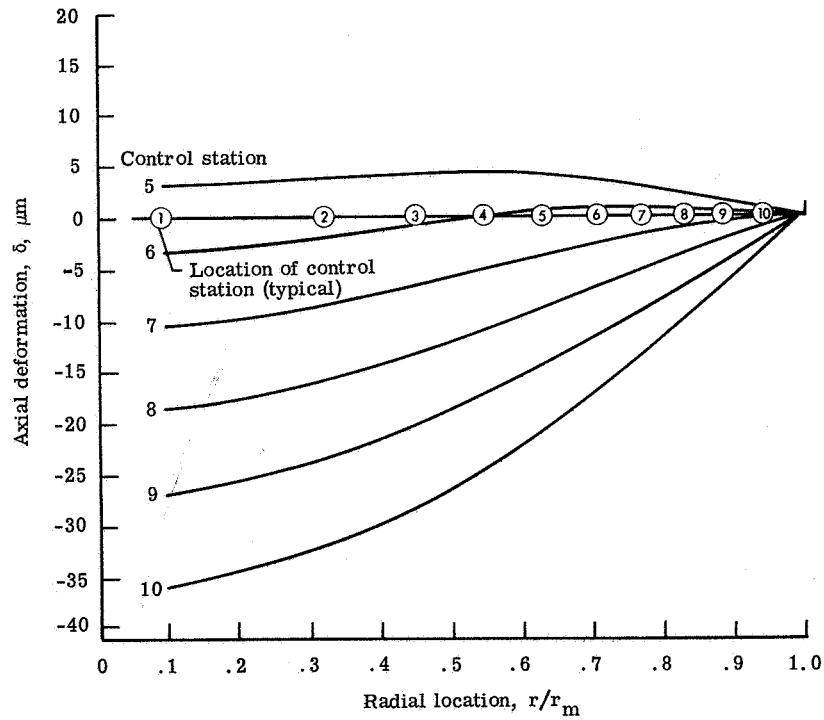
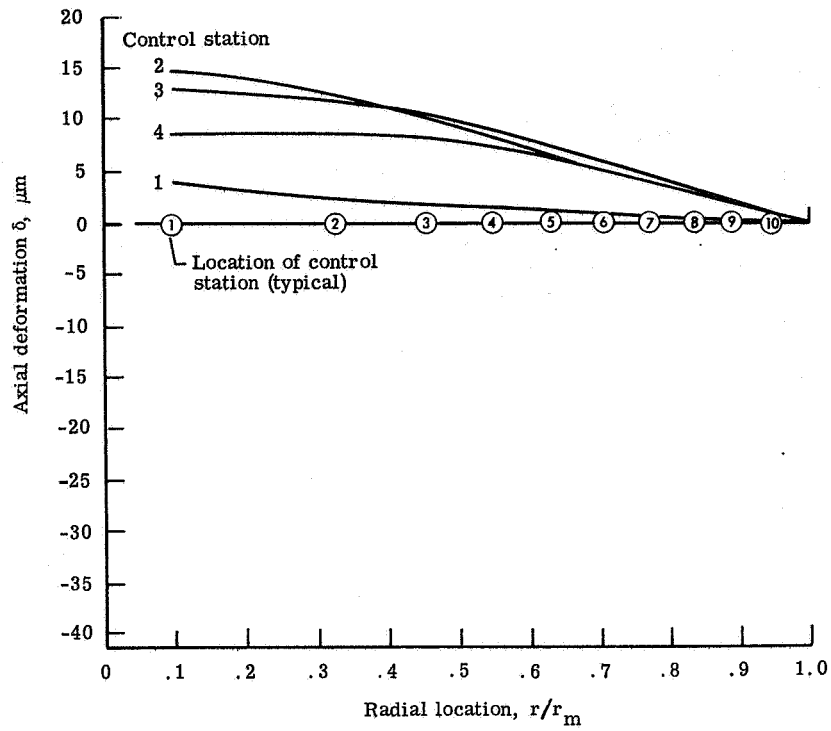


Figure 6.- Axial deformation due to unit amplitude thermal input applied individually at equal area spacing.

coefficient matrices were inverted and the resulting stiffness matrices give the amplitude of the thermal input necessary to correct a given set of axial deflections at the control stations. In addition to the amplitude of the thermal input, the accuracy of the amplitude necessary for diffraction-limited operation may be determined. This accuracy is given by the product of the minimum contribution (minimum coefficient k_{ij}) and the maximum allowable error, $\delta_a = 0.05 \mu\text{m}$. An examination of the stiffness matrices indicates that the amplitude A of the thermal input must be controlled to within 1.0 mK for the case of equal meridional spacing and to within 0.23 mK for equal area spacing in order to insure diffraction limited operation. For either configuration the sensitivity of the deformations makes it necessary to employ a closed-loop control system to maintain the proper contour. Since the thermal inputs for the equal meridional spacing have lower control requirements, this spacing configuration is the preferred configuration of the two considered herein.

Constant Acceleration Loading

To illustrate the use of the thermal active optics system the deformation due to a constant acceleration loading was examined. The axial deflection due to a 0.01g acceleration load was determined by using the computer program of reference 13. The axial deformation as a function of radial location for this load is shown in figure 7. For this relatively light loading the maximum axial deflection exceeds the tolerance limit indicated in the figure by a factor of about 25. In order to correct this distortion it is necessary to introduce a deformation of equal magnitude and opposite sign by use of the thermal loads. By using the deformation of the 0.01g loading, the amplitude of the corrective thermal loads was determined from equation (4) for the case of equal meridional

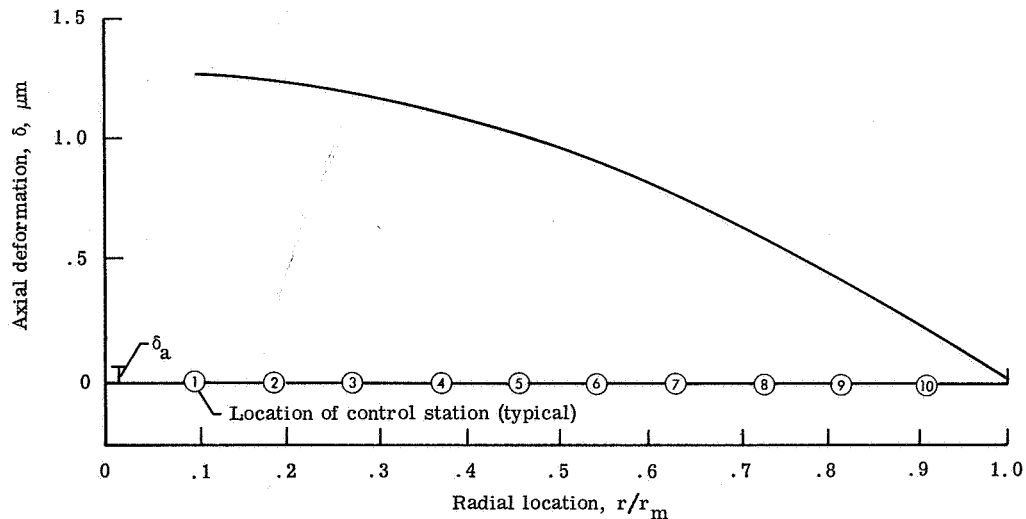


Figure 7.- Axial deformation of beryllium telescope mirror due to 0.01g constant acceleration load. $f = 12.0 \text{ m}$.

spacing. Then the computer program was used to determine the resulting displacement with both the acceleration load and the corrective thermal loads applied. The resulting deformation is shown in figure 8. Also indicated in the figure is the amplitude of the thermal input applied to each control point. The residual deformation is well within the tolerance limit; however, the deformation does not go to zero at all control points as might be expected. The residual deformation at the control points is due to errors introduced by the matrix inversion process and roundoff of the thermal inputs. It is significant that only low amplitude thermal inputs are necessary to correct deformations which exceed the tolerance limit by such a large amount.

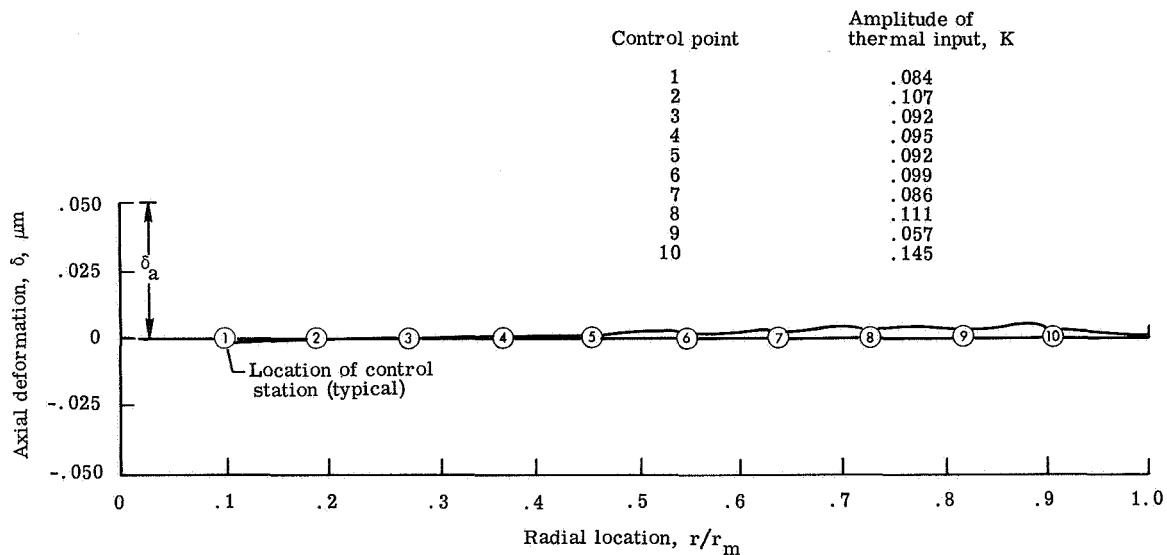


Figure 8.- Axial deformation of beryllium telescope mirror subjected to 0.01g constant acceleration load and corrective thermal inputs. $f = 12.0$ m.

CONCLUDING REMARKS

An analysis for correcting axial deformations in a thin telescope mirror has been investigated. This analysis would be used in conjunction with a closed-loop control system to thermally correct surface deformations. The analysis has been demonstrated on a thin beryllium paraboloid with a focal length to diameter ratio of 4. Two patterns of control points for symmetrical thermal inputs were examined. To correct axisymmetric deformations the amplitude of the temperature distribution must be controlled to within 1.0 mK for equal meridional spacing and to within 0.23 mK for equal area spacing. For either configuration the sensitivity of the deformations makes it necessary to employ a closed-loop control system to maintain the proper contour. Since the equal meridional spacing has a lower control requirement it is the preferred configuration of the two considered.

Deformations due to a constant acceleration load were examined and were found to exceed the allowable tolerance level by a factor of about 25. It was found that these deformations were readily corrected to well within the required accuracy by using relatively small amplitude thermal inputs.

Langley Research Center,
National Aeronautics and Space Administration,
Hampton, Va., November 27, 1972.

APPENDIX A

SHELL-GEOMETRY SUBROUTINES

The subroutine INPUT necessary to calculate the shell geometry for the computer program of reference 13 is as follows:

```

SUBROUTINE INPUT(NMAX)
COMMON R(502)/BL1/GAM(502),OMT(502),OMXI(502),DEOMX(502)/BL3/NU,
1LAM,N,EALSIG,CHAR,DEL
READ(5,1)S,F,R(1)
1 FORMAT(3F10.5)
DEL=S/(CHAR*FLOAT(NMAX-2))
K=1
A=CHAR
NTLAS=NMAX-1
IF(R(1).EQ.0.0000) 2,3
2 GAM(1)=1.E321
GO TO 4
3 GAM(1)=1./(R(K)*SQRT(R(K)**2*A**2/(4.*F**2)+1.))
4 OMT(1)=1./SQRT(4.*F**2/A**2+R(K)**2)
OMXI(1)=4.*A*F**2/(4.*F**2+A**2*R(K)**2)**1.5
DEOMX(1)=-24.*A**3*R(K)*F**3/(4.*F**2+A**2*R(K)**2)**3
CALL SURFAC(2,F,0.5*DEL)
DO 5 K=3,NTLAS
CALL SURFAC(K,F,DEL)
5 CONTINUE
CALL SURFAC(NMAX,F,0.5*DEL)
DO 6 K=2,NMAX
GAM(K)=1./(R(K)*SQRT(R(K)**2*A**2/(4.*F**2)+1.))
OMT(K)=1./SQRT(4.*F**2/A**2+R(K)**2)
OMXI(K)=4.*A*F**2/(4.*F**2+A**2*R(K)**2)**1.5
6 DEOMX(K)=-24.*A**3*R(K)*F**3/(4.*F**2+A**2*R(K)**2)**3
RETURN
END

```

APPENDIX A

The subroutine SURFACE called by the subroutine INPUT is given as follows with the necessary function subprogram:

```
SUBROUTINE SURFAC(K,F,DELTA)
COMMON R(502)/BL3/NU,LAM,N,EALS1G,CHAR,DEL
REAL K1,K2,K3,K4
K1=DELTA*VALUE(R(K-1),F,CHAR)
K2=DELTA*VALUE(R(K-1)+0.5*K1,F,CHAR)
K3=DELTA*VALUE(R(K-1)+0.5*K2,F,CHAR)
K4=DELTA*VALUE(R(K-1)+K3,F,CHAR)
R(K)=R(K-1)+(1./6.)*(K1+2.*K2+2.*K3+K4)
RETURN
END
```

```
FUNCTION VALUE(P,F,CHAR)
C=2.*F
D=SQRT(P*P*CHAR*CHAR+4.*F*F)
VALUE=C/D
RETURN
END
```

APPENDIX B

SUBROUTINE FORCE

The corrected subroutine FORCE for the computer program of reference 13 is given as follows:

```

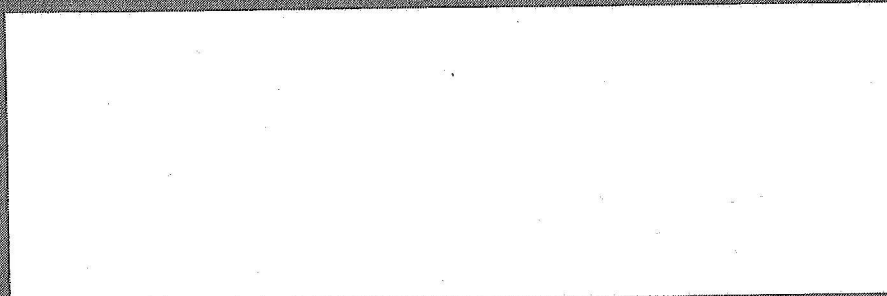
      SUBROUTINE FORCE(K,IND5,NMAX)
C SUBROUTINE FORCE THIS SUBROUTINE CALCULATES THE ELEMENTS OF THE LOWER CASE
C E-VECTOR AS DEFINED IN APPENDIX A OF REFERENCE(12), AT THE STATION SPECIFIED
C BY THE INDEX K.
      COMMON R(502)/BL1/GAM(502),OMT(502),OMXI(502),DEOMX(502)/BL3/NU,
      1LAM,N,EALSIG,CHAR,DEL/BL4/CEE(4)
      REAL NU,LAM,N,L2
      REAL MSTP
      RA=R(K)
      GA=GAM(K)
      OX=OMXI(K)
      OT=OMT(K)
      T=TEMP(K,DEL)

      DT=DTEMP(K,DEL)
      DELT1=DELT(K,DEL)
      DLT1=DDELT(K,DEL)
      PX1=PX(K,DEL)
      PT1=PT(K,DEL)
      P1=P(K,DEL)
      H=HHT(K,DEL)
      DH=DHHT(K,DEL)
      HRB=HRA(K,DEL)
      DHRB=DHRA(K,DEL)
      D1=1.-NU
      L2=LAM**2
      EAL=EALSIG
      TSUBT=2.*H*EAL/(D1*HRB)*T
      MSTP=CHAR*EAL/(3.*D1)*((1.5/HRB-3./HRB**2+2./HRB**3)*(DLT1*H**3+3.
1H**2*DH*DELT1)+DELT1*H**3*DHRB/HRB**2*(-1.5+6./HRB-6./HRB**2))
      CEE(4)=CHAR*EAL*DELT1*H**3/(3.*D1)*(1.5/HRB-3./HRB**2+2./HRB**3)
      CEE(1)=-PX1+2.*EAL/(D1*HRB)*(H*DT+T*DH)-DHRB/HRB*TSUBT-
1L2*D1*GA*OX*CEE(4)
      CEE(2)=-PT1-N/RA*TSUBT-L2*D1*N/RA*OT*CEE(4)
      CEE(3)=-P1-(OX+OT)*TSUBT-L2*D1*GA*MSTP+
1L2*D1*CEE(4)*(OX*OT-(N/RA)**2)
      RETURN
      END

```


REFERENCES

1. Kopal, Zdenek: Tasks for the Manned Orbital Telescope. *Astronaut. & Aeronaut.*, vol. 3, no. 12, Dec. 1965, pp. 16-21.
2. Spitzer, Lyman, Jr.; and Boley, Bruno A.: Thermal Deformations in a Satellite Telescope Mirror. *J. Opt. Soc. Amer.*, vol. 57, no. 7, July 1967, pp. 901-913.
3. Anon.: A System Study of a Manned Orbital Telescope. D2-84042-1 (Contract NAS1-3968), Boeing Co., Oct. 1965. (Available as NASA CR-66047.)
4. Anon.: Technology Study for a Large Orbiting Telescope. 70-9443-1 (Contract NASw-1925), Opt. Syst. Div., Itek Corp., May 15, 1970. (Available as NASA CR-110253.)
5. Anon.: Optical Technology Apollo Extension System - Phase A. Vol. III, Sec. III. Contract NAS 8-20256, Space Div., Chrysler Corp., Oct. 18, 1967. (Available as NASA CR-90303.)
6. Robertson, Hugh J.: Development of an Active Optics Concept Using a Thin Deformable Mirror. NASA CR-1593, 1970.
7. Couder, André: Thermal Distortions of Telescope Mirrors and Their Correction. *Vistas in Astronomy*, Vol. 1, Arthur Beer, ed., Pergamon Press, 1955, pp. 372-377.
8. Comm. on Metric Pract.: ASTM Metric Practice Guide. NBS Handbook 102, U.S. Dep. Com., Mar. 10, 1967.
9. Creedon, Jeremiah F.: Discrete Control of Linear Distributed Systems With Application to the Deformable Primary Mirror of a Large Orbiting Telescope. Ph. D. Thesis, Univ. of Rhode Island, 1970.
10. Barnes, W. P., Jr.: Considerations in the Use of Beryllium for Mirrors. *Appl. Opt.*, vol. 5, no. 12, Dec. 1966, pp. 1883-1886.
11. Sanders, J. Lyell, Jr.: An Improved First-Approximation Theory for Thin Shells. NASA TR R-24, 1959.
12. Budiansky, Bernard; and Radkowski, Peter P.: Numerical Analysis of Unsymmetrical Bending of Shells of Revolution. *AIAA J.*, vol. 1, no. 8, Aug. 1963, pp. 1833-1842.
13. Schaeffer, Harry G.: Computer Program for Finite-Difference Solutions of Shells of Revolution Under Asymmetric Loads. NASA TN D-3926, 1967.
14. Platt, Robert J., Jr.; and Rhodes, Marvin D.: Thermal Distortion of a Paraboloidal Shell. NASA TN D-6471, 1971.



POSTMASTER: If Undeliverable (Section 138
Postal Manual) Do Not Return

"The aeronautical and space activities of the United States shall be conducted so as to contribute . . . to the expansion of human knowledge of phenomena in the atmosphere and space. The Administration shall provide for the widest practicable and appropriate dissemination of information concerning its activities and the results thereof."

—NATIONAL AERONAUTICS AND SPACE ACT OF 1958

NASA SCIENTIFIC AND TECHNICAL PUBLICATIONS

TECHNICAL REPORTS: Scientific and technical information considered important, complete, and a lasting contribution to existing knowledge.

TECHNICAL NOTES: Information less broad in scope but nevertheless of importance as a contribution to existing knowledge.

TECHNICAL MEMORANDUMS: Information receiving limited distribution because of preliminary data, security classification, or other reasons.

CONTRACTOR REPORTS: Scientific and technical information generated under a NASA contract or grant and considered an important contribution to existing knowledge.

TECHNICAL TRANSLATIONS: Information published in a foreign language considered to merit NASA distribution in English.

SPECIAL PUBLICATIONS: Information derived from or of value to NASA activities. Publications include conference proceedings, monographs, data compilations, handbooks, sourcebooks, and special bibliographies.

TECHNOLOGY UTILIZATION PUBLICATIONS: Information on technology used by NASA that may be of particular interest in commercial and other non-aerospace applications. Publications include Tech Briefs, Technology Utilization Reports and Technology Surveys.

Details on the availability of these publications may be obtained from:

SCIENTIFIC AND TECHNICAL INFORMATION OFFICE

NATIONAL AERONAUTICS AND SPACE ADMINISTRATION

Washington, D.C. 20546